Rotational Mobility of Guest Molecules in *o*-Terphenyl below T_g

S. Yu. Grebenkin* and B. V. Bol'shakov

Institute of Chemical Kinetics and Combustion, Novosibirsk 630090, Russian Federation

Received: December 23, 2005; In Final Form: March 12, 2006

An optical anisotropy decay technique for measuring probe rotational times in glassy materials is presented. Rotational times from $10^{1.4}$ to 10^5 s have been obtained for a molecule of 1-naphthyl-azomethoxybenzene (NAMB) in *o*-terphenyl (OTP) over a temperature range from T_g +3.5 to T_g −16.5 K. The rotational diffusion follows the temperature dependence of Debye−Stokes−Einstein down to T_g −4 K with an activation energy of 320 ± 30 kJ/mol. Below T_g −9 K, the temperature dependence of rotation mobility was found to be much weaker with an activation energy of 70 ± 15 kJ/mol.

1. Introduction

Serious efforts were made to characterize molecular dynamics in condensed matter near and below the glass transition temperature T_g.[1−3] It is established that the dynamic properties of amorphous solids (viscosity, diffusion) change drastically as the system is cooled to T_g.

Although the glass-forming materials have been studied extensively, the nature of molecular motions near and below T_g remains unclear. Many processes (chemical reactions, rotation of molecules) that appear as an exponential decay in liquids may become highly nonexponential near and below glass transition because of spatially heterogeneous dynamics.[1−5] The time evolution of processes is often well described by the Kohlrausch−Williams−Watts (KWW) equation

$$f(t) = f(0)\exp(-t/\tau)^{\beta} \qquad (1)$$

or can be represented by the sum of two (or more) exponentials.[4,6,7]

The rotation of impurity molecules was studied extensively in many solvents. When the size of a solute molecule is larger or comparable with that of a solvent, the rotational diffusion coefficient frequently follows the temperature dependence of Debye−Stokes−Einstein at temperatures above T_g:

$$D_{rot} = \frac{1}{6\tau_c} = \frac{kT}{8\pi\eta r^3} \qquad (2)$$

where τ_c is the rotational correlation time, η is the viscosity, and r is the hydrodynamic radius of a rotating particle. This relationship holds for a great number of compounds over a wide temperature range. For example, the rotation of probe molecules in *o*-terphenyl (OTP) follows this law over the rotational time range of 14 orders of magnitude.[8,9]

Single-molecule spectroscopy was used to study the rotational diffusion of rhodamine 6G in OTP just above the glass transition.[10] During short periods of time, motion of molecules in each environment is the Brownian rotation process characterized by a single correlation time.

Below T_g, the rotational mobility of molecules is poorly known. The ESR method was used[11] to investigate the rotational dynamics of the spin probe 2,2,6,6-tetramethylpiperidinoxyl (TEMPO) in OTP and phenyl salicylate (SALOL). The η/T temperature dependence of rotational correlation time was found down to $T \sim 1.25\ T_g$. In OTP, it is proportional to $(\eta/T)^{\chi}$ with $\chi < 1$ in the range from 280 to 298 K. Below 280 K, the temperature dependence of rotational time is depicted in the Arrhenius plot by two straight lines with the point of intersection at 235 K. The activation energy was found to be approximately 15 kJ/mol above and 5 kJ/mol below T_g. A small value of rotational correlation time obtained at low temperatures ($\sim 2 \times 10^{-8}$ s at 235 K) is questionable.

The rotation of probe molecules in OTP near and above T_g was measured by using the photobleaching technique and the time-correlated single-photon counting method.[8,9,12−14] The probe size is either almost the same as that of the OTP molecule or larger. The kinetics of rotational motion obeys the law of eq 1. The rotation of probes follows temperature dependence described by eq 2 down to 238 K.

The aim of this work is to study the rotational mobility of probe molecules in OTP at temperatures below T_g. OTP is the typical fragile glass-forming liquid, attractive because of both its relatively simple structure and stability as a supercooled liquid. The literature data on OTP glass temperature give values in the range of 243−246 K. We take a value of 243 K measured by the calorimetric method.[15] Molecular dynamics at low temperatures in this substance has been studied by single-molecule spectroscopy,[10] photobleaching technique,[8,9,12−14] dielectric relaxation,[16] NMR,[5] and ESR.[11,17]

In the present work, we have used 1-naphthyl-azomethoxybenzene (NAMB) as a probe molecule. Under light irradiation, NAMB undergoes cis−trans isomerization. The linearly polarized light creates the anisotropic orientational distribution of probe molecules in a sample. The light-induced anisotropy of samples was observed as a linear dichroism which relaxes in the dark. The rate of dark *cis*−*trans* isomerization is negligibly low in the temperature range used.

2 Experimental Section

2.1. Experimental Setup. The anisotropy decay kinetics were monitored by measuring sample absorbance (spectrophotometer SPECORD UV−Vis, Carl Zeiss JENA) at a wavelength of absorption maximum of trans isomer (388 nm). The design of the spectrophotometer allowed us to obtain absorbance values in the digital form. The experimental setup is schematically depicted in Figure 1.

* Corresponding author. E-mail: grebenk@ns.kinetics.nsc.ru.

10.1021/jp057487o CCC: $33.50
Published on Web 04/07/2006

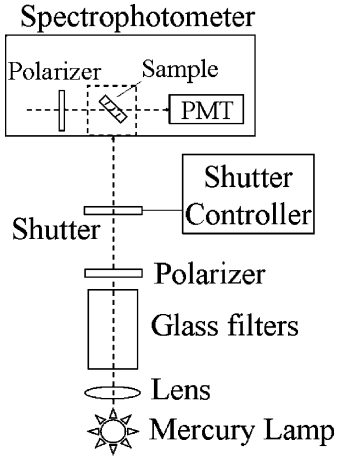

Figure 1. Schematic representation of the experimental setup. Projection onto the horizontal plane.

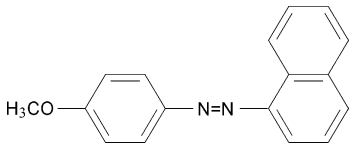

Figure 2. The chemical structure of NAMB.

The temperature-controlled aluminum cell (temperature controller Polikon 613, Thermex, S.-Petersburg), equipped with quartz windows for a probe and irradiation light beams, was placed in the spectrophotometer. It was cooled by gaseous nitrogen evaporated in a Dewar flask and passed through the channels drilled in the cell walls. The sample temperature was kept constant to within ±0.1 K. The measuring accuracy of temperature was ±0.3 K.

A 500 W high-pressure mercury arc lamp (DRSh-500-2M) powered by direct current was used as a source of irradiation. Light of wavelength 405 nm was isolated by the standard set of glass filters immersed into a water bath. The typical photon flux at 405 nm measured by the rate of azobenzene photo isomerization in isooctane[18] was $(3.9 \pm 0.4) \times 10^{16}$ photon s^{-1} cm^{-2}.

The polarized light was obtained by using polarizers from LOMO PLC. To polarize a probe beam, the polarizer was installed directly behind the probe light source inside the spectrophotometer. A homemade holder allows two fixed positions of the polarizer at which the probe light has either vertical or horizontal polarization. Because of light attenuation (by the polarizer), a more powerful incandescent lamp of 50 W (Royal Philips Electronics) was used as the probe light source. It takes about two seconds to change manually the polarizer orientation.

2.2. Sample Preparation. The OTP powder (Fluka, ≥99.0% (GC), mp 329−332 K) was used as received. The azo dye NAMB was synthesized in our laboratory as described in ref 19 and used after thin-layer chromatography purification. Its chemical structure is depicted in Figure 2.

The OTP powder was placed in a Pyrex glass ampule with a rectangular cross-section of 1 mm × 8 mm and a height of 15 mm. The OTP was melted in the ampule, and then the azo dye was dissolved there. The typical concentration of NAMB in solution was about 4×10^{-4} mol/l.

The ampule with a solution was kept at 373−393 K during 1.5 h. After that, no crystallization of OTP was observed at room temperature for several months.

After heating, the ampule has been kept at room temperature for 3 min and then placed into the cell cooled to the experimental temperature. The samples obtained did not crack and contained no bubbles. The ampule was mounted in the cell so that the angles between the light beams and the plane with a face of 15 mm × 8 mm were 45° (Figure 1). After 17 h exposure at the experimental temperature in the dark, the sample was irradiated with a vertically polarized light at 405 nm for 90 min to create optical anisotropy. The anisotropy decay kinetics was measured after irradiation.

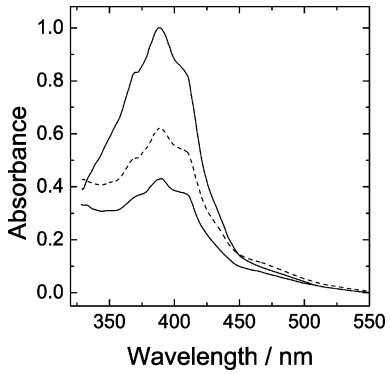

Figure 3. UV−Vis absorption spectrum of NAMB in OTP before irradiation (top curve) and after 0.5 h of irradiation with vertically polarized light of wavelength 405 nm (middle and bottom curves), 239 K. The polarization of the probe light is horizontal (middle curve) and vertical (bottom curve).

3. Results and Discussion

3.1. The Temperature Dependence of Rotational Mobility. Figure 3 shows the spectra of the optical absorption of NAMB in OTP before and after exposure to the polarized light of a wavelength of 405 nm. Light irradiation leads to a decrease in sample absorption over the trans isomer absorption range. As follows from the figure, upon irradiation with vertically polarized light, the sample absorption spectrum depends on the probing light polarization. The figure clearly demonstrates the appearance of optical absorption anisotropy upon cis−trans isomerization.

A quantitative description of experimental data was performed by using the value of sample anisotropy that we define as

$$A(t) = \frac{\mathrm{Abs}_{\perp}(t) - \mathrm{Abs}_{||}(t)}{2\mathrm{Abs}_{\perp}(t) + \mathrm{Abs}_{||}(t)} \qquad (3)$$

where $\mathrm{Abs}_{\perp}$ and $\mathrm{Abs}_{||}$ are the absorbances of the sample at 388 nm measured by using the horizontal and vertical polarizations of probing light, respectively. As follows from eq 3, the $A(t)$ value is one-third of the difference in $\mathrm{Abs}_{\perp}$ and $\mathrm{Abs}_{||}$ values normalized to isotropic absorbance.

Figure 4 shows the typical curves of anisotropy decay in the dark. The data for 226.5 and 236.5 K were collected in single experiments. The decay curve at 246.5 K was obtained by averaging the data of 12 individual experiments. In the last case, the accumulation of data is necessary due to the high rate of signal decay, which causes a large measurement error.

Figure 5 demonstrates the constancy of isotropic sample absorbance, $(2\mathrm{Abs}_{\perp}(t) + \mathrm{Abs}_{||}(t))/3$, in the course of anisotropy decay. The figure plots the isotropic sample absorbance normalized to its time-averaged value, $\langle 2\mathrm{Abs}_{\perp}(t) + \mathrm{Abs}_{||}(t)\rangle/3$, vs time. This constancy confirms that the rotation of the NAMB molecules is the only process which is monitored.

Figure 4 shows that the KWW equation describes satisfactorily the anisotropy decay curves. At 246.5 K, β is close to unity and the kinetics of anisotropy decay obeys the exponential

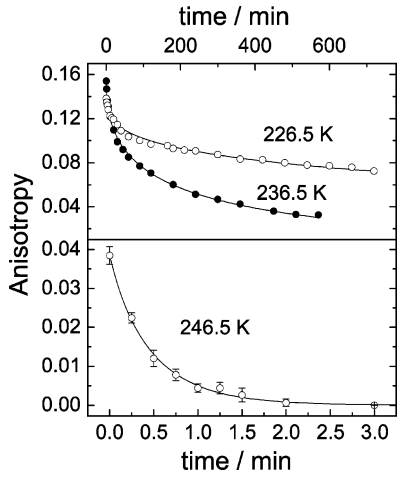

Figure 4. Anisotropy decay curves at different temperatures. Solid lines are the KWW stretched exponential fits to the data. The error bar is one standard deviation.

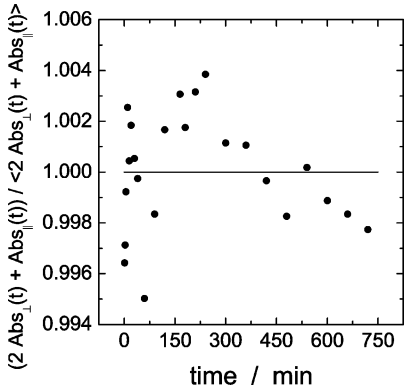

Figure 5. The constancy of the isotropic sample absorbance during anisotropy decay, 226.5 K. The line indicates the time average.

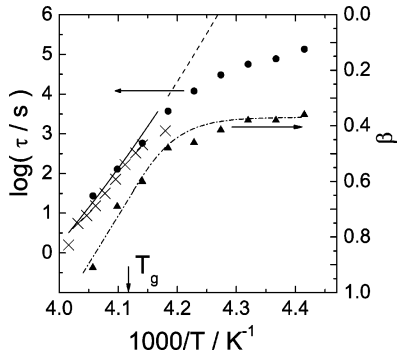

Figure 6. The Arrhenius plot of rotational times (solid circles) and the temperature dependence of stretched exponential parameter β (triangles) for NAMB in OTP. Crosses: rotational correlation times for tetracene in OTP.[8] The solid line is the VFTH approximation of η/T for neat OTP,[20] shifted vertically. The dashed line is the extrapolation of VFTH equation into the low-temperature region. The dashed−dotted line is the guide for the eye.

dependence. The temperature dependence of rotational times follows η/T down to $T_g - 4$. There are no experimental data on the OTP viscosity value at lower temperatures.

Figure 6 shows (dashed line) the extrapolation of the η/T using the Vogel−Fulcher−Tamman−Hesse (VFTH) equation for relaxation time

$$\tau = A \exp\frac{B}{T - T_0} \qquad (4)$$

The comparison between relaxation time and η/T is motivated by eq 2. To this end, we used the VFTH equation, with the parameters based on the viscosity data over the range of 238−294 K.[20] The figure shows the decoupling of the values of rotational times and calculated viscosity in the lower temperature range (T < 239 K). For the temperatures above 239 K, the effective activation energy of rotational diffusion is 320 ± 30 kJ/mol, which is equal to the activation energy of α relaxation, 320 kJ/mol, measured in OTP at 251 K.[16] Such a high value is, probably, due to the collective character of rotational mobility. At temperatures below 234 K, the activation energy of NAMB rotation is 70 ± 15 kJ/mol. This value exceeds the activation energy of Johari−Goldstein secondary relaxation in OTP (50 kJ/mol) observed in this temperature range.[16]

The temperature dependence curve of NAMB rotation in OTP changes the slope near 236.5 K which is 6.5 K as low as T_g. Note that, ref 11, the knee of the temperature dependence of TEMPO rotation in OTP was revealed near 235 K. However, the type of molecular mobility presented in ref 11 is not quite clear.

The KWW equation parameter β can be considered as a measure of the width of molecule distribution over rotational times. A wider distribution corresponds to a smaller β value. The β decreases sharply in the range of 239−246.5 K. At temperatures below 239 K, it depends only weakly on temperature. A decrease in temperature near T_g also leads to an increase in the dispersion of the rotation rates of rhodamine 6G in OTP.[10]

The values of rotational times at temperatures higher than 236.5 K are in good agreement with the data of Ediger and co-workers on the rotation of tetracene in OTP.[8] For example, at 241.5 K, the rotational times presented in ref 8 and, measured in the present work, are 520 and 580 s, respectively. At 246.5 K, these values are 14 and 27 s, respectively. For comparison, the data of work[8] are shown in Figure 6.

3.2. Manifestation of Heterogeneity in Optical Anisotropy Decay. The biexponential law

$$A(t) = W_f \exp(-t/\tau_f) + W_s \exp(-t/\tau_s) \qquad (5)$$

can be successfully used to describe the nonexponential kinetics of optical anisotropy decay over the temperature range of 226.5−244 K. The parameters with the indexes f and s refer to the fast and slow exponentials.

By solving the problem of diffusion on a sphere, we get the time dependence of anisotropy for a homogeneous medium:[21]

$$A(t) = A(0) \exp(-6D_{rot}t) \qquad (6)$$

The NAMB particle is not spherical. Therefore, strictly speaking, the rotational diffusion coefficients for rotation around the three principal axes are different.[22,23] Moreover, the anisotropy decay results from the rotation of two NAMB isomers, which vary in size, and hence have different mobilities. By irradiating the sample with polarized light of various wavelengths, we formed anisotropy at different isomer ratios. Irradiating with a light of 405 and 546 nm yields cis isomer portions of 60 and 20%, respectively. Only a slight difference was observed in the kinetics of anisotropy decay after sample irradiation with the polarized light of the wavelengths listed. Therefore, we conclude that the rotational times for cis and trans isomers are close. For the same reason, we assume that there is no great difference in rotational diffusion coefficients for the rotation around various principal axes. Otherwise, because of the strongly different geometry of cis and trans molecules, the decay kinetics would strongly depend on isomer ratio. It is

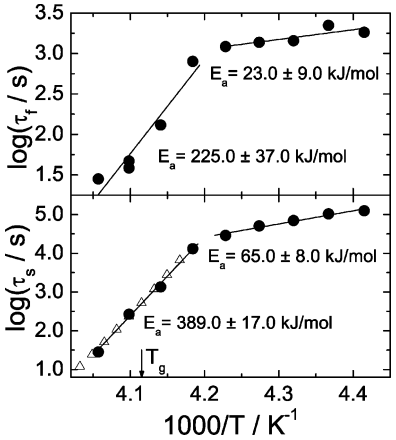

Figure 7. Temperature dependencies of rotational times, τ_f and τ_s (circles). Triangles: temperature dependence of η/T for neat OTP,[20] shifted vertically. The solid lines are the results of τ_f and τ_s fitting in low- and high-temperature regions using the Arrhenius equation.

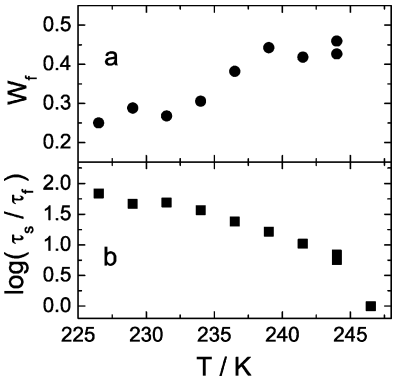

Figure 8. Temperature dependence of the parameters of bimodal distribution over rotational times: the fraction of rapidly rotating particles (a) and the effective width of distribution (b).

assumed then that a heterogeneity of matrix is the main reason for nonexponential anisotropy decay.

Thus, the anisotropy decay kinetics can be interpreted as particle rotation in the surroundings of two types. Figure 7 shows the temperature dependencies of τ_f and τ_s. The parameters were determined by fitting the curves of anisotropy decay by using eq 5. The slopes of the curves change in the vicinity of 239 K. As it is shown in Figure 6, the slope of the temperature dependence curve of the KWW parameter τ changes also near 239 K. Figure 7 demonstrates good agreement between the temperature dependence of η/T (data of work[20]) and that of τ_s. Thus, at temperatures higher than 239 K, the rotation of guest molecules in low-mobility regions follows the temperature dependence of η/T. At the same time, the rotation in high-mobility regions at $T > 239$ K decreases with decreasing temperature to a much lesser extent than η/T.

Activation energies of rotational times were evaluated in low- (226.5−236.5 K) and high-temperature (239−246.5 K) parts of the measured temperature range. These values are listed in Figure 7. Recall that the activation energy of β relaxation in the range 205−237 K is equal to 50 kJ/mol.[16]

Figure 8 shows the temperature dependencies of a fraction of rapidly rotating particles, W_f, and of the value $\log(\tau_s/\tau_f)$. The latter reflects the width of particle distribution over rotational times. The values τ_f, τ_s, and W_f are weakly dependent on the temperature below 235 K. Probably, this is due to the fact that the local matrix structure does not change substantially with decreasing temperature below this point.

Note that, at temperatures 241.5 and 244 K, the rotational times of "fast" molecules are so small that they compare with anisotropy formation time. Therefore, at mentioned temperatures, the values W_f are not equal to the portions of NAMB molecules located in high-mobility regions and should be considered as lower bounds of these portions.

Reducing the entire range of rotation times to two values simplifies the real situation. Moreover, this model does not take into account an interconversion of fast and slow regions that may arise from environment rearrangement. In the high-temperature region, these processes could play a great role. Nevertheless, this simple model can be used to draw two conclusions. First, a fraction of high-mobility regions decreases with decreasing temperature. Second, with decreasing temperature, the particle rotation in the low-mobility regions becomes slower to a greater extent than in the high-mobility regions.

4. Conclusions

In this paper, we have presented a photo orientation technique to measure the long rotational correlation times of probe azo molecules in glassy materials. The results obtained for rotational times over the range of $10^{1.4}-10^5$ s are given. The technique can be also used to measure longer times. The measurements of probe molecules rotation in glassy OTP provide the data extended to temperatures down to T_g −16.5 K.

We have found that the rotational diffusion of probe molecules follows the temperature dependence of Debye−Stokes−Einstein down to T_g −4 K. Below this temperature, the temperature dependence of rotational mobility is much slower. An activation energy of 70 ± 15 kJ/mol was determined below T_g −4 K.

Acknowledgment. We thank Alexander Alturmesov for production of ampules. This work was supported by the Russian Foundation for Basic Research, project no. 03-03-33125.

References and Notes

(1) Angell, C. A.; Ngai, K. L.; McKenna, G. B.; McMillan, P. F.; Martin, S. W. *J. Appl. Phys.* **2000**, *88*, 3113.
(2) Ngai, K. L. *J. Non-Cryst. Solids* **2000**, *275*, 7.
(3) Ediger, M. D. *Annu. Rev. Phys. Chem.* **2000**, *51*, 99.
(4) Tolkatchev, V. A. Kinetics of the Simplest Radical Reactions in Solids. In *Reactivity of Solids: Past, Present and Future. JUPAC. A Chemistry for 21st Century*; Boldyrev, V. V., Ed.; Blackwell Science: Oxford, 1996, p 185.
(5) Bohmer, R.; Chamberlin, R. V.; Diezemann, G.; Geil, B.; Heuer, A.; Hinze, G.; Kuebler, S. C.; Richert, R.; Schiener, B.; Sillescu, H.; Spiess, H. W.; Tracht, U.; Wilhelm, M. *J. Non-Cryst. Solids* **1998**, *235−237*, 1.
(6) Stracke, A.; Bayer, A.; Zimmermann, S.; Wendorff, J. H.; Wirges, W.; Bauer-Gogonea, S.; Bauer, S.; Gerhard-Multhaupt, R. *J. Phys. D: Appl. Phys.* **1999**, *32*, 2996.
(7) Brown, D.; Natansohn, A.; Rochon, P. *Macromolecules* **1995**, *28*, 6116.
(8) Cicerone, M. T.; Ediger, M. D. *J. Phys. Chem.* **1993**, *97*, 10489.
(9) Cicerone, M. T.; Blackburn, F. R.; Ediger, M. D. *J. Chem. Phys.* **1995**, *102*, 471.
(10) Deschenes, L. A.; Vanden Bout, D. A. *J. Phys. Chem.* **2002**, *106*, 11438.
(11) Andreozzi, L.; Bagnoli, M.; Faetti, M.; Giordano, M. *J. Non-Cryst. Solids* **2002**, *303*, 262.
(12) Cicerone, M. T.; Ediger, M. D. *J. Chem. Phys.* **1992**, *97*, 2156.
(13) Cicerone, M. T.; Ediger, M. D. *J. Chem. Phys.* **1995**, *103*, 5684.
(14) Wang, C.-Y.; Ediger, M. D. *J. Phys. Chem.* **1999**, *103*, 4177.
(15) Greet, R. J.; Turnbull, D. *J. Chem. Phys.* **1967**, *46*, 1243.
(16) Johari, G. P.; Goldstein, M. *J. Chem. Phys.* **1970**, *53*, 2372.
(17) Vorobiev, A. Kh.; Gurman, V. S.; Klimenko, T. A. *Phys. Chem. Chem. Phys.* **2000**, *2*, 379.
(18) Zimmerman, G.; Chow, L.; Paik, U. *J. Am. Chem. Soc.* **1958**, *80*, 3528.

(19) Becker, H.; Berger, W.; Domschke, G.; Fanghanel, E.; Faust, J.; Fischer, M.; Gentz, F.; Gewald, K.; Gluch, R.; Mayer, R.; Muller, K.; Pavel, D.; Schmidt, H.; Schollberg, K.; Schwetlick, K.; Seiler, E.; Zeppenfeld, G. *Organicum*, 15th ed.; VEB Deutscher Verlag der Wissenschaften: Berlin, 1976.

(20) Laughlin, W. T.; Uhlmann, D. R. *J. Chem. Phys.* **1972**, *76*, 2317.

(21) Carrington, A.; McLachlan, A. D. *Introduction to Magnetic Resonance with Applications to Chemistry and Chemical Physics*; Harper & Row: New York, Evanston, and London, 1967.

(22) Brocklehurst, B.; Young, R. N. *J. Phys. Chem. A* **1999**, *103*, 3809.

(23) Brocklehurst, B.; Young, R. N. *J. Phys. Chem. A* **1999**, *103*, 3818.